



**BNL-95140-2011-CP**

***Warm Magnetic Field Measurements of LARP HQ  
Magnet***

**X. Wang, S. Caspi, D. Cheng, D. Dietderich, H. Felice, P.  
Ferracin, R. Hafalia, J. Joseph, J. Lizarazo, M. Martchevskii, C.  
Nash, G.L. Sabbi, C. Vu, LBNL Berkeley, CA 94720, U.S.A.  
J. Schmalzle, P. Wanderer, BNL, Upton, NY 11973, U.S.A.  
G. Ambrosio, R. Bossert, G. Chlachidze, J. DiMarco, V.  
Kashikhin, FNAL, Batavia, IL 60510, U.S.A.**

*Presented at the Particle Accelerator Conference (PAC11)  
New York City, NY  
March 28 – April 1, 2011*

May 2011

**Superconducting Magnet Division**

**Brookhaven National Laboratory**

**U.S. Department of Energy  
DOE Office of Science**

Notice: This manuscript has been authored by employees of Brookhaven Science Associates, LLC under Contract No. DE-AC02-98CH10886 with the U.S. Department of Energy. The publisher by accepting the manuscript for publication acknowledges that the United States Government retains a non-exclusive, paid-up, irrevocable, world-wide license to publish or reproduce the published form of this manuscript, or allow others to do so, for United States Government purposes.

This preprint is intended for publication in a journal or proceedings. Since changes may be made before publication, it may not be cited or reproduced without the author's permission.

## **DISCLAIMER**

This report was prepared as an account of work sponsored by an agency of the United States Government. Neither the United States Government nor any agency thereof, nor any of their employees, nor any of their contractors, subcontractors, or their employees, makes any warranty, express or implied, or assumes any legal liability or responsibility for the accuracy, completeness, or any third party's use or the results of such use of any information, apparatus, product, or process disclosed, or represents that its use would not infringe privately owned rights. Reference herein to any specific commercial product, process, or service by trade name, trademark, manufacturer, or otherwise, does not necessarily constitute or imply its endorsement, recommendation, or favoring by the United States Government or any agency thereof or its contractors or subcontractors. The views and opinions of authors expressed herein do not necessarily state or reflect those of the United States Government or any agency thereof.

# WARM MAGNETIC FIELD MEASUREMENTS OF LARP HQ MAGNET\*

X. Wang<sup>†</sup>, S. Caspi, D. Cheng, D. Dietderich, H. Felice, P. Ferracin, R. Hafalia, J. Joseph, J. Lizarazo, M. Martchevskii, C. Nash, G.L. Sabbi, C. Vu, LBNL, Berkeley, CA 94720, U.S.A.  
J. Schmalzle, P. Wanderer, BNL, Upton, NY 11973, U.S.A.

G. Ambrosio, R. Bossert, G. Chlachidze, J. DiMarco, V. Kashikhin, FNAL, Batavia, IL 60510, U.S.A.

## Abstract

The US-LHC Accelerator Research Program is developing and testing a high-gradient quadrupole (HQ) magnet, aiming at demonstrating the feasibility of Nb<sub>3</sub>Sn technologies for the LHC luminosity upgrade. The 1 m long HQ magnet has a 120 mm bore with a conductor-limited gradient of 219 T/m at 1.9 K and a peak field of 15 T. HQ includes accelerator features such as alignment and field quality. Here we present the magnetic measurement results obtained at LBNL with a constant current of 30 A. A 100 mm long circuit-board rotating coil developed by FNAL was used and the induced voltage and flux increment were acquired. The measured  $b_6$  ranges from 0.3 to 0.5 units in the magnet straight section at a reference radius of 21.55 mm. The data reduced from the numerical integration of the raw voltage agree with those from the fast digital integrators.

## INTRODUCTION

As part of the US-LHC Accelerator Research Program (LARP), Fermilab (FNAL), Brookhaven National Laboratory (BNL), and Lawrence Berkeley National Laboratory (LBNL) collaborate on developing Nb<sub>3</sub>Sn superconducting quadrupole magnets for the LHC luminosity upgrade. Following the technology quadrupole (TQ) and long quadrupole (LQ) programs [1, 2], the high-gradient quadrupole (HQ) magnets represent another step towards this goal. With a bore size of 120 mm, the 1 m long HQ has a maximum gradient of 199 T/m with short-sample current of 17.7 kA at 4.4 K [3]. HQ magnets include accelerator magnet features such as alignment and field quality [3, 4]. Here we report the observations during the warm measurement of HQ01d at LBNL. Experimental setup is presented, followed by the measurement results and discussion.

## EXPERIMENTAL DETAILS

### Setup

The magnet was positioned vertically in the test cryostat with the lead side on the top. Inside the magnet bore was an anti-cryostat housing the rotating probe developed by FNAL (Fig. 1). The nominal bore size of the anticryostat is 49 mm and the length is 2.3 m. Two coils, one 100 mm long

and the other 250 mm long, were installed in the probe. The distance between the center of the two coils is  $\sim 250$  mm.



Figure 1: The circuit-board probe used in the measurement. The 100 mm coil is close to the left end.

Unlike the conventional rotating coil based on windings wound on a cylindrical mandrel, the coil used here consists of traces on a circuit board. More details about this novel design can be found in [5]. The radius of the outermost trace is  $\sim 21.55$  mm. Each coil has three voltage outputs, i.e., unbucked (UB), dipole-bucked (DB) and dipole-quadrupole-bucked (DQB) signals, which were amplified by an onboard amplifier inside the probe during the measurement. The probe rotated at a speed of  $\sim 0.5$  Hz. In every revolution, a chain of 4096 quadrature pulses and one index pulse were generated by an incremental encoder mounted at the end of the probe. The probe movement along the bore direction ( $z$ ) was controlled by a step motor with a resolution of  $\sim 2 \mu\text{m}$  [6].

Data was acquired by a hybrid system composed of a dynamic signal acquisition card (National Instruments DSA 4472B), two fast digital integrators (Metrolab FDI 2056), and other auxiliary cards. All three probe voltage signals and the encoder signals were simultaneously acquired by the DSA card. Only the UB and DQB signals were acquired by the FDI cards. The DSA and FDI cards have amplifiers at their input end. The nominal gains used at each amplifier stage are listed in Table 1.

Table 1: Nominal gains for the voltage signals.

Amplifier	UB	DB	DQB
Probe	10	10	1000
DSA	1	1	1
FDI	100	-	50

The sampling of the DSA card was driven by its internal clock at a frequency of 102.4 kHz. The quadrature signal from the encoder triggered the FDI cards. The magnet current and probe temperature were measured by an NI 6221 card. The PXI-based data acquisition system was controlled by a LabWindows/CVI program.

\* This work was supported by the U.S. Department of Energy through the US LHC Accelerator Research Program.

<sup>†</sup> xrwang@lbl.gov

## Measurement Protocol

The measurements were performed at  $\sim 70$  K during the warmup of the magnet from 4.5 K. A constant current of 30 A was applied. Once the current was stabilized, the probe took measurements at different locations along the magnet length. Typical step size ranged from 10 mm close to the coil end to 50 mm in the straight section. Five measurements (rotations) were taken at each location. The averaged harmonics are reported with the error bars indicating the maximum and minimum values of the five measurements. The measured results are compared to the calculation given by an Opera 3D model of the magnet where the coil and structural components were considered. A typical one-way scan of 35  $z$  locations took  $\sim 45$  minutes. The magnet terminal voltage and the strain gage readings were monitored to ensure minimal temperature rise.

## RESULTS AND DISCUSSION

### Data reduction

The 2D complex bore field is expanded as

$$B_y + i B_x = \sum_{n=1}^{\infty} \vec{C}_n \left( \frac{x + iy}{R_{\text{ref}}} \right)^{n-1}, \quad (1)$$

where  $\vec{C}_n$  is complex multipole coefficients defined at the reference radius  $R_{\text{ref}}$ . The normalized coefficients  $\vec{c}_n$  reported here is defined as  $\vec{c}_n = b_n + i a_n = 10^4 \vec{C}_n / B_2$ , where  $B_2$  is the main field of the quadrupole magnet with zero main skew component ( $A_2 = 0$ ). Here we use  $R_{\text{ref}} = 21.55$  mm, 35% of the bore radius. The flux data as a function of angular position used to generate the  $\vec{C}_n$  is a running sum of the flux increments over angular steps of the probe indicated by the encoder quadrature signal [7]. For the DSA voltage data, the flux increment is obtained by numerically integrating the recorded voltage over the time interval defined by two consecutive quadrature signals from the encoder with the same polarity. For the FDI cards, the flux increments are readily available as the instrument output. Before the normalization, flux drift is removed due to the stable magnet current [7]. The probe centering correction is done based on the first 10 orders of harmonic coefficients, assuming the dipole components shown in the recorded UB signal were only due to the probe offset in a quadrupole field.

### Transfer Function

The measured main-field transfer function along the bore are compared to the calculation (Fig. 2). The measurement was done with the 100 mm coil. The UB signal is used in this case as DB signal was not recorded for the FDI card. The theoretical value was calculated with  $I = 50$  A.

Magnetic center is located at  $z = 0$  in Fig. 2. Lead side of the magnet is at right ( $z > 0$ ) and the return side at left. Limited by the length of the anti-cryostat, the measurements did not cover the return side. Between  $-200$

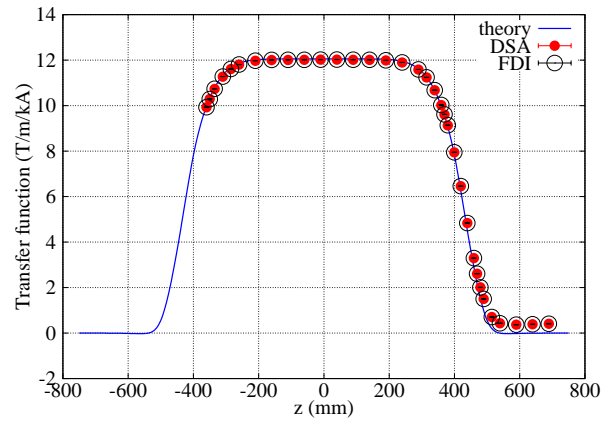


Figure 2: Axial dependence of main field ( $B_2$ ) transfer function measured at  $\sim 70$  K with  $I = 30$  A using the 100 mm coil.

mm and 200 mm, the transfer function reaches a plateau  $\sim 12$  T/m/kA. The discrepancy between the measurement and calculation becomes evident for  $z > 460$  mm, where less than half of the 100 mm rotating coil is within the magnet coil. The residual value is  $\sim 0.4$  T/m/kA for  $z > 600$  mm, corresponding to  $\sim 250$   $\mu$ T at the reference radius of 21.55 mm. The five measurements taken at each location were close to each other, leading to the invisible error bars in Fig. 2. Typical variation of the measurements at each location is less than 0.03%. The measured data from DSA and FDI agree well. Typical difference is less than 0.1% for  $z < 400$  mm and less than 0.3% for  $z > 400$  mm.

### Allowed harmonics

Figure 3 compares the axial dependence of  $b_6$  normalized to  $B_2(z = 0)$ . The data was reduced from the DQB signal of the 100 mm coil.

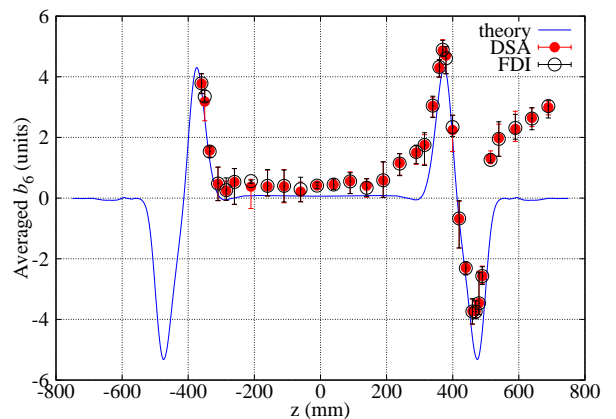


Figure 3: Axial dependence of  $b_6$  measured at  $\sim 70$  K with  $I = 30$  A using the 100 mm coil. Results normalized to the central  $B_2$ .  $R_{\text{ref}} = 21.55$  mm.

The measured data generally agrees with the calculation with a few exceptions. First, based on the measured  $b_6$ ,

one sees that actual straight section of the magnet ranges between  $\sim -200$  mm and 100 mm. The increasing of the measured  $b_6$  between 100 mm and 300 mm may be due to the transition turn from the inner layer to the outer layer of the coil that is not considered in the present calculation and will be addressed in future models. Second, the deviation of the measurements from the calculation is noticed for  $z > 460$  mm, which can be related to the residual  $B_2$  at the same location as shown in Fig. 2. This could be due to the fact that the 2D bore field assumption is not true at the coil end.

$b_6$  ranges from 0.3 to 0.5 units in the straight section ( $-200 < z < 100$  mm) at  $R_{\text{ref}} = 21.55$  mm. The error bar length is  $\sim 0.5$  units. Given the 2D field in the straight section, the scaling based on Eq. (1) gives a  $b_6$  ranging from 1.5 to 2.5 units at  $R_{\text{ref}} = 30$  mm, 50% of the magnet bore radius.

Figure 4 shows the axial dependence of  $b_{10}$  normalized to  $B_2(z = 0)$ . Due to the limited signal/noise ratio, the measured data spread around the calculated values. Nevertheless, the measured results are within  $\pm 0.2$  units with a stable variation within  $\pm 0.4$  units.

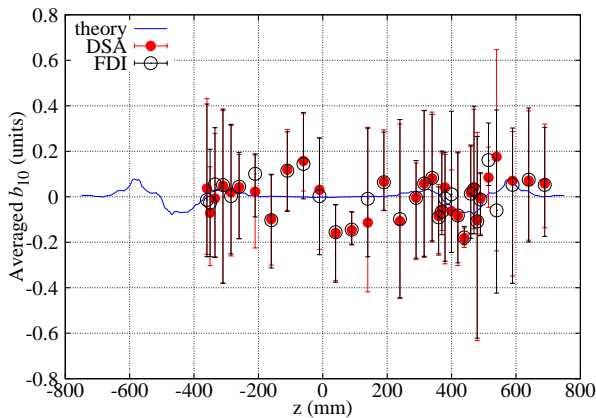


Figure 4: Axial dependence of  $b_{10}$  measured at  $\sim 70$  K with a current of 30 A using the 100 mm coil. Results normalized to the central  $B_2$ .  $R_{\text{ref}} = 21.55$  mm.

### Comparison between DSA and FDI

The hybrid system allows the comparison between the two methods to acquire the angular flux data for field quality analysis as mentioned previously. From Figs. 2 to 4, one sees that the data reduced from two methods are in excellent agreement in terms of both averaged values and their variation. This indicates that for the measurement scenario reported here, i.e., a probe rotation speed of 0.5 Hz vs. a DSA sampling rate of 102.4 kHz (a factor of  $2 \times 10^5$ ), the numerical integration based on the trapezoidal rule with linear interpolation between the recorded voltage data achieves a performance comparable to the fast digital integrator. With the raw voltage recorded by the DSA, it is possible to postprocess the raw voltage, e.g., digital filtering, to reach potentially higher signal/noise ratio for the

analysis. Since the FDI cards used their front-end amplifier in addition to the onboard amplifier inside the probe (Table 1), the agreement between the DSA and FDI results suggests that the FDI gains were accurate.

## SUMMARY

Warm magnetic measurements of HQ01d, a high-gradient  $\text{Nb}_3\text{Sn}$  quadrupole, were performed at LBNL with a constant current of 30 A and a temperature of 70 K. The measured data given by the rotating circuit-board coil developed at FNAL are in good agreement with the calculation. A transfer function of  $\sim 12$  T/m/kA is measured at the straight section of the magnet. At a reference radius of 21.55 mm, the measured  $b_6$  ranges between 0.3 to 0.5 units in the straight section. This scales to 1.5 to 2.5 units at a reference radius of 30 mm, 50% of the magnet bore radius. The measurement also compares the performance of the flux data construction based on the numerical integration of the recorded voltage and the fast digital integrator. The agreement between the two methods indicates that the setup and the associated integration technique is effective for the measurement involving DC measurement with slowly rotating probes.

## ACKNOWLEDGMENTS

We thank the technical staff of the program for their expertise and dedicated support. We also thank B. Richter of GMW Associates and P. Keller of Metrolab for the loan of two fast digital integrators and their help during the system setup.

## REFERENCES

- [1] H. Felice *et al.*, “Test results of TQS03: A LARP shell-based  $\text{Nb}_3\text{Sn}$  quadrupole using 108/127 conductor.” *Journal of Physics: Conference Series*, 234(3):032010, 2010.
- [2] G. Ambrosio *et al.*, “Test results of the first 3.7 m long  $\text{Nb}_3\text{Sn}$  quadrupole by LARP and future plans.” *IEEE Trans. Appl. Supercond.*, 2011. In press.
- [3] S. Caspi *et al.*, “Design of a 120 mm bore 15 T quadrupole for the LHC upgrade phase II.” *IEEE Trans. Appl. Supercond.*, 20(3):144–147, 2010.
- [4] H. Felice *et al.*, “Magnetic and mechanical analysis of the HQ model quadrupole designs for LARP.” *IEEE Trans. Appl. Supercond.*, 18(2):281–284, 2008.
- [5] J. DiMarco, “Rotating circuit board probes for magnetic measurements.” The 15th Internal Magnetic Measurement Workshop, Fermilab, August 2007, <http://tdserver1.fnal.gov/immw15/>.
- [6] J. Joseph *et al.*, “Magnetic measurement DAQ system specification.” Document # 40Y570, Superconducting Magnet Program, LBNL, December 2008.
- [7] L. Bottura, “Standard analysis procedures for field quality measurement of the LHC magnets — part I: harmonics.” Technical Report LHC-MTA-IN-97-007, LHC/MTA, 2001.